

INVESTIGATION OF THE INTERANNUAL VARIABILITY OF THE TROPICAL ATLANTIC OCEAN FROM SATELLITE DATA

Sabine Arnault and Jean Luc Melice

LOCEAN UMR CNRS/IRD/UPMC/MNH, Paris, FRANCE

(Marine Geodesy, 2012)

Abstract : The low frequency (interannual) variability of the tropical Atlantic Ocean is analyzed with series of altimetric dynamic topography data, sea surface temperatures, and wind stress between Octobre 1992 and January 2011 using Empirical Orthogonal Functions and Singular Value Decompositions. Three regions of maximum variability are evidenced: a northern one, between 10 and 20°N, where altimetry, sea surface temperature and wind stress are strongly connected through thermosteric and Ekman pumping effects in particular in 2010 but also in 1998 and in 2005; A southern region, along 20°S, where dynamic topography decreases in particular in 1997 and in 2010 in agreement with surface cooling and southern tradewinds intensification; An equatorial region whose variability appears either as an Est-West slope of the topography and temperature all along the equator (2005 and 2010) or as a (cold) tongue in the Gulf of Guinea (1997 and 2002). Both local wind (meridional component) and western remote (zonal component) effects can be involved in this oceanic triggering. First results of the teleconnections between this tropical Atlantic interannual variability and the tropical Pacific El Niño–Southern Oscillation indicate a possible connection of the tropical Atlantic between 10-20°N with a 19 weeks delay, and in the Gulf of Guinea with a 70-80 weeks one.

I. DATA SETS AND METHODS

Altimetric data (ADT)

AVISO merged Ssalto/Duacs Absolute Dynamic Topography (ADT) merged products.
Resolutions : weekly from October 1992 to January 2011, 1/3° x 1/3° from 30°N to 30°S, 60°W and 20°E.
(<http://www.aviso.oceanobs.com>)

Sea Surface Temperature (SST)

Optimally interpolated (re)analysis by Reynolds et al. (2002).
Resolutions : weekly from October 1992 to January 2011, 1° x 1° from 30°N to 30°S, 60°W and 20°E.
(http://www.emc.ncep.noaa.gov/research/cmb/sst_analysis)

Wind stresses

European Center for Medium Range Weather Forecasts (ECMWF) ERA-interim reanalysis wind stresses data.
Resolutions : 6h from October 1992 to January 2011, 0.75°x 0.75° from 30°N to 30°S, 60°W and 20°E.
(<http://www.ecmwf.int/research/era/do/get/era-interim>)

All these series have been interpolated in space and in time to get weekly 1°x1° files and a low-pass wavelet transform filter has been applied to remove all oscillations with periods shorter than or equal to 12 months.

Methods

Empirical Orthogonal Functions and Singular Value Decomposition (EOF and SVD) analysis

II. TROPICAL ATLANTIC ADT LOW-FREQUENCY VARIABILITY

First EOF ADT (Fig. 1) :

- opposition between the region 20°N-15°S and the other areas
- 64% of the variance between 10-15°N, 25-45°W, and between 25-30°N, 30-60°W
- oscillations about 2 years (around 2000) and 5-6 years (1993-1998 and 2004-2010) on the corresponding Principal Component (PC) confirmed by Wavelet analysis (CWT)

Second EOF ADT (Fig. 2) :

- located in the south-western, 2 opposite extrema : 25-30°S, 10-40°W, and 10-15°S, 10-30°W
- corresponding correlations around 0.7
- year to year fluctuations with maximum amplitude between 2005-2011. Peaks also in boreal winter 1999-2000

Third EOF ADT (Fig. 3) :

- structure similar to the equatorial upwelling with a "tongue" in the Gulf of Guinea ($r=0.6-0.8$)
- PC is mainly negative, peaks in 2001-2003 (extremum), in early 1997 and in 2010 (weakest signal) => equatorial upwelling more intense. Conversely, ADT slightly higher than usual in late 1998 and between 2003-2009
- 4-5 year periods indicated by CWT between 1998 and 2003

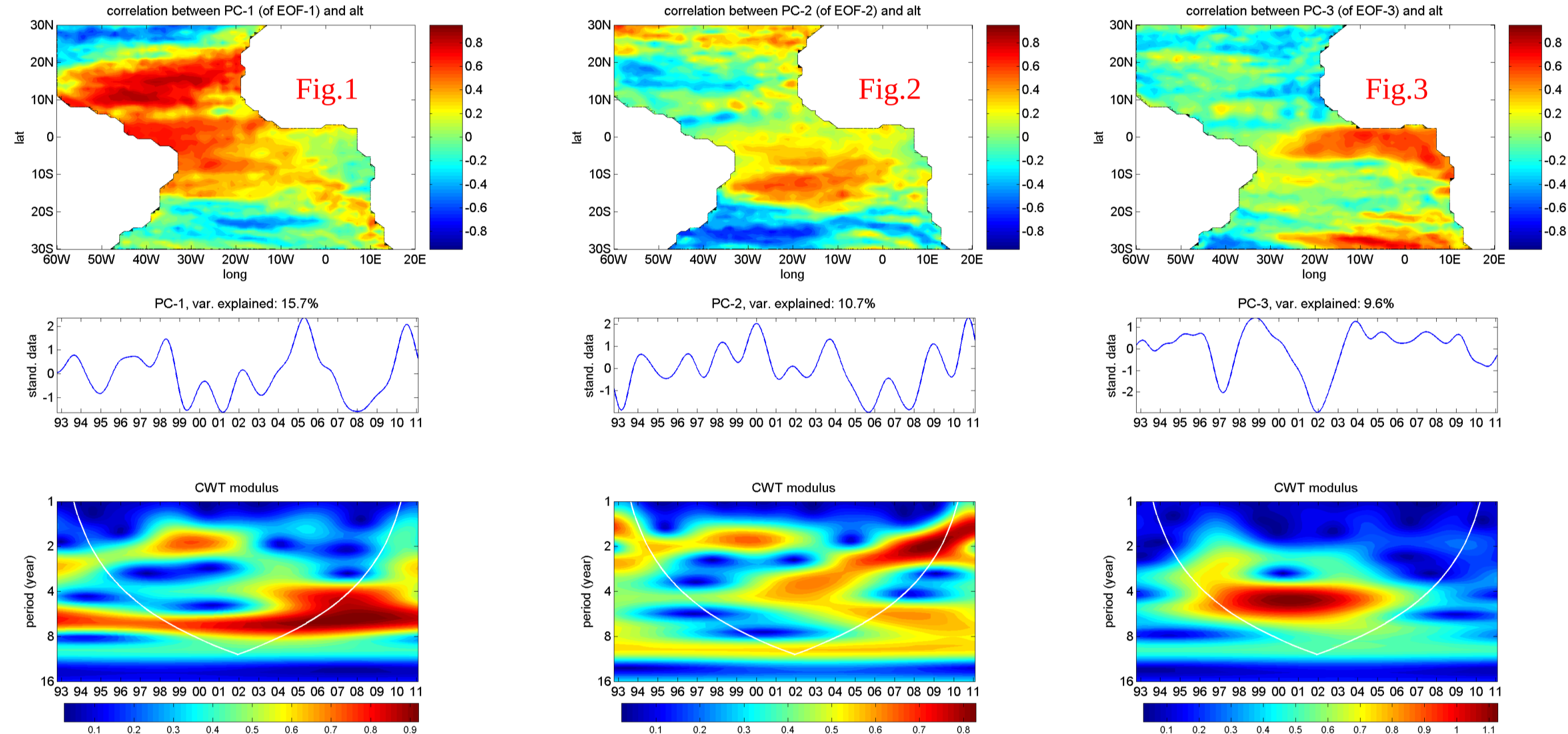


Fig. 1-3: Homogeneous correlation map of the first, second and third EOF of the low-frequency altimetric ADT data (top). Color scale is from $r=[-1, 1]$. Corresponding PC series from October 1992 until July 2011 (middle). Continuous Wavelet Transform (CWT) modulus of the PC of the first, second and third EOF (bottom). The oscillations observed outside the cone of influence (white line), should be interpreted with caution.

First SVD ADT/wind stress (Fig. 7) :

- 51% of the scf, $r=0.79$
- structures concern the tradewinds in the northern hemisphere, especially off the African coast
- ADT structures similar to the first EOF
- correlation SVD scores/first EOF PCs = 0.98 for the wind and 0.93 for ADT
- These results express the connection between the strengthening/weakening of the northern tradewinds and the corresponding increase/decrease of the local ADT with a few month lags (the winds lead). The relationship holds mostly during the last part of the series with the remarkable events in early 2005 and 2010. The wind stress relaxation in the Northern basin is then connected with an ADT increase along 10-20°N. The SVD performed between the wind stress curl and the ADT (not shown) reveals that this oceanic response in the north tropical Atlantic basin is due to the Ekman pumping process associated with the wind stress curl modifications during these periods. Along the equator, the wind increase in the West is associated with the ADT zonal slope strengthening.

Second SVD ADT/wind stress (Fig. 8) :

- 12 % of the scf
- extrema located in the southern basin for the wind, altimetric variability along the equator, and in the southwestern Atlantic in the region of the SMW between 15 and 25°S as already observed in the second SVD (ADT/SST)
- series shows extreme negative values during the ends of 1997 and 2009, and in early 2003 : ADT increases in the southern MSW region and equatorial slope strengthens. Positive extrema in 2005 when the situation reverses
- $r=0.82$ => a strong coupling between the wind stress and the ADT during these events
- contrary to the first SVD, no relationship with wind stress curl is observed

Fourth SVD ADT/wind stress (Fig. 9) :

- reveals the interesting structure shown by the ADT third EOF in the Gulf of Guinea
- 8.5% of the scf
- correlation between the scores = 0.79 with major events in 1997 and between 2001 and 2003 => ADT decrease in the Gulf of Guinea due to local wind action as the southerlies increase.

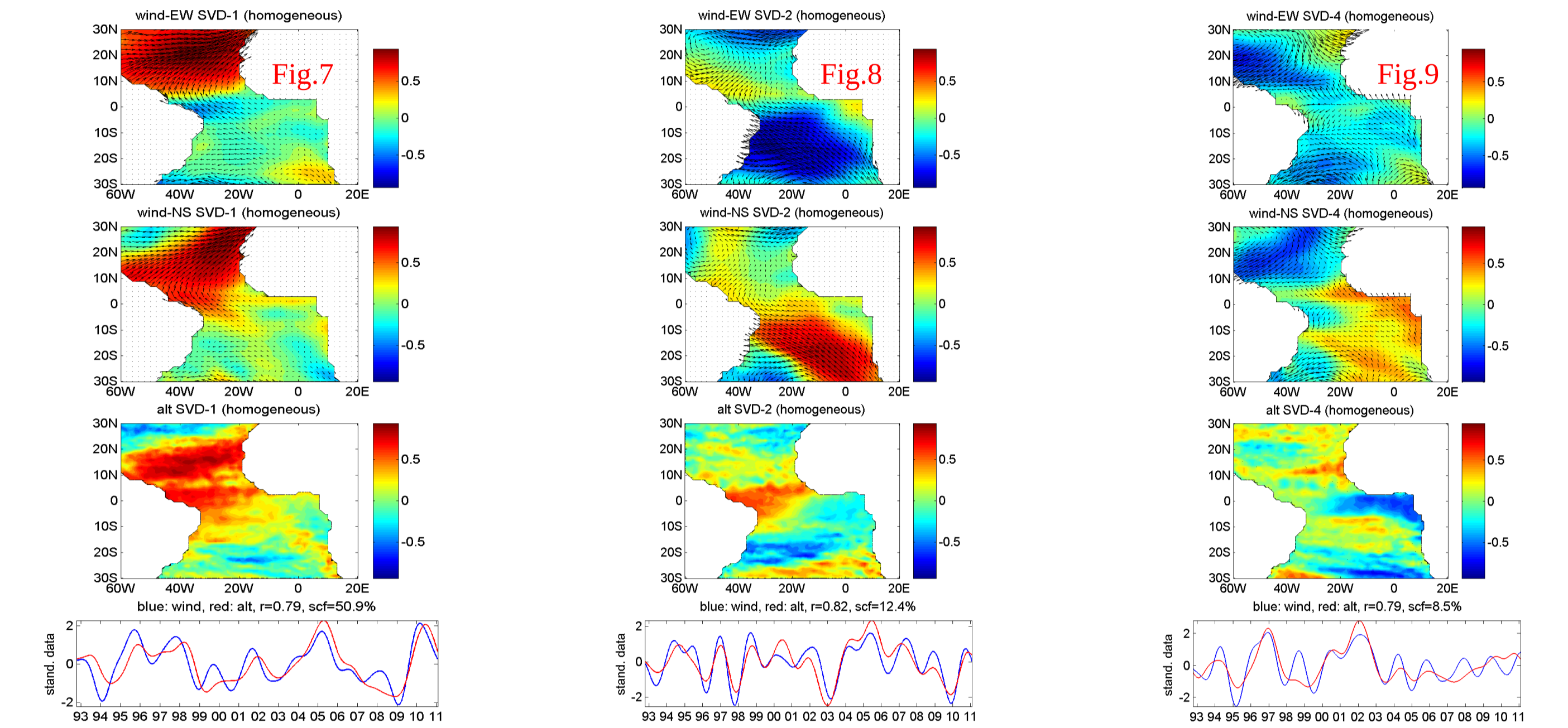


Fig. 7-9: Homogeneous correlation maps of the τ^x and τ^y components of the first, second and fourth SVD of the low-frequency altimetry ADT and wind stress data (map for τ^x followed by map for τ^y , top). The colors correspond to the correlation between the altimetry data and τ^x and τ^y . The arrows are the SVD output of the wind-altimetry SVD analysis in which the wind components are not treated independently. Homogeneous correlation map of the altimetry ADT component of the first, second and third SVD of the low-frequency altimetry ADT and wind stress data (middle). Color scale is from $r=[-1, 1]$. Corresponding SVD scores for ADT (red) and wind stress (blue) (bottom).

IV. RELATION WITH PACIFIC EL NIÑO

3 events dominate the Pacific SST structures during our time series : the 1997-1998 "eastern" Niña, the 1998-99 "central" Niña, and then the 2008-2010 "central" Niña-Niña.

First SVD tropical Pacific SST/tropical Atlantic wind stress (Fig. 10) and ADT (fig. 11) :

- scf > 70%
- scores show only 2 events: the ENSOs in 1997-98 and in 2009-10
- Pacific SST SVD shows a tongue of warm waters extending from the American coast out to 160°E, simultaneous Atlantic tradewinds weaken except in the western equatorial zone (strong τ^x anomaly), high ADT concentrated along 10-20°N
- correlations between the respective PCs and scores = 0.71 (ADT) and = 0.88 (winds).

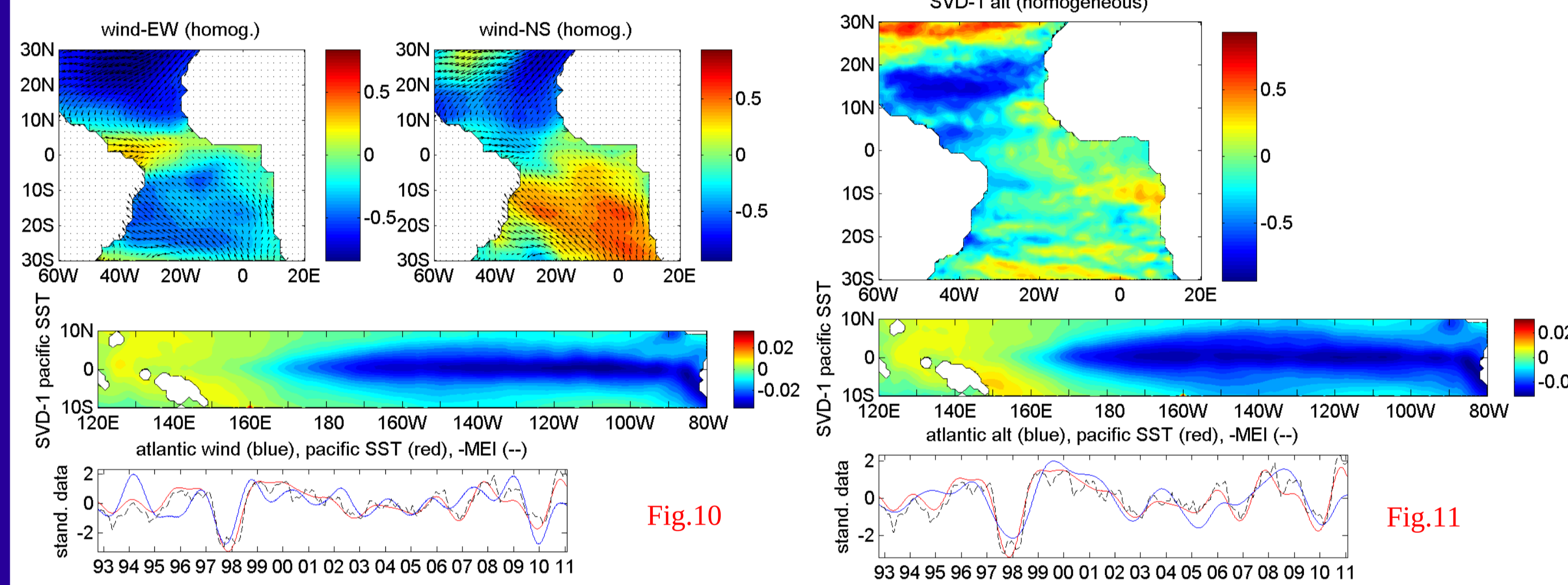


Fig. 10: Homogeneous correlation maps of the tropical Atlantic wind stress τ^x and τ^y components of the first SVD of the low-frequency Atlantic wind stress and Pacific SST data (map for τ^x followed by map for τ^y , top). The SVD-obtained wind arrows are superimposed. Homogeneous correlation map of the tropical Pacific SST component of the first SVD of the low-frequency Atlantic wind stress and Pacific SST data (middle). Corresponding SVD scores for SST (red) and wind stress (blue) (bottom). The MEI index with sign inverted is also displayed (dotted black curve).
Fig. 11: Same as Figure 10, except for the Atlantic altimetric ADT data.

We explore the lagged relationships. We calculate the first SVD between these two fields at n lags from 1 to 104 weeks (2 years, Pacific SST leads the Atlantic ADT). The best correlation ($r=0.80$) is obtained at 19 weeks (4 months) for the first EOF PC. This delay scheme and the regions involved (North Atlantic) are in agreement with Enfield and Mayer (1997)'s results. The same computations with the third EOF PC (associated with the Gulf of Guinea upwelling) results in a delay of 70 weeks ($r=0.91$). Such a lag of 16 months is in agreement with Tourre and White (2005)'s results. The SVD between the Atlantic altimetry, Atlantic winds and the Pacific SST at these lags are displayed in Fig. 12 and 13, respectively.

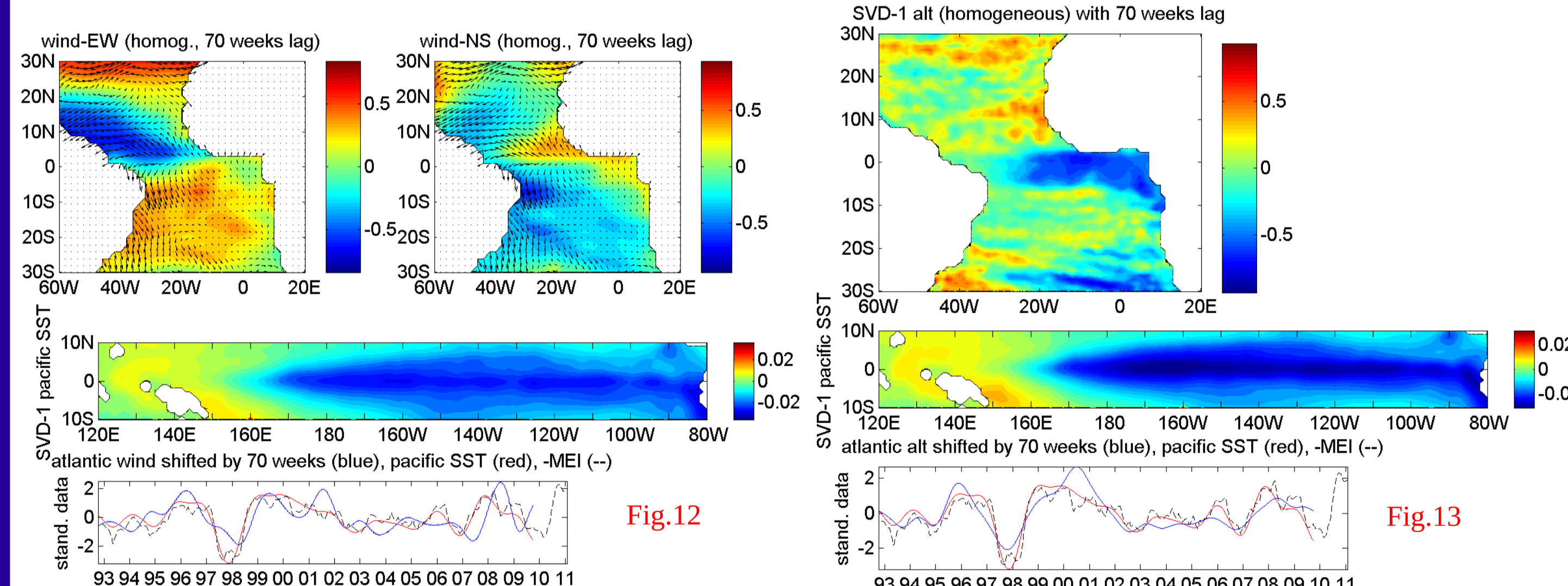


Fig. 12: Same as Figure 10, except for an SVD analysis with lag in which the Pacific SST leads the Atlantic altimetric data by 70 weeks. For reason of visual comparison between the signals, the Atlantic altimetry score is shifted in time by 70 weeks.
Fig. 13: Same as Figure 11, except for an SVD analysis with lag in which the Pacific SST leads the Atlantic wind by 70 weeks. For reason of visual comparison between the signals, the Atlantic wind score is shifted in time by 70 weeks.

CONCLUSIONS

This statistical analysis based on satellite altimetry, SST and modeled wind stress in the tropical Atlantic is successful in showing coherent and related interannual variability of the fields from 1992 until 2011, in particular between 10 and 20°N, and in the equatorial region. Simple physical concepts can explain common features such as an increase in ADT and an increase in SST connected through thermosteric effects to a weakening of the tradewinds in the northern Atlantic in 2010. The same relationship can be found in 1998 and in 2005, but with a smaller intensity. Conversely, for a long period lasting from 2007 until early 2009, a tradewind intensification is associated with a cooling and a decrease in ADT. In the southern region, ADT decreases in particular in 1997 and in 2010 in agreement with SST cooling and southern trade intensification, and increases in 1998, 2003 and 2009 with inverse relationship. However, the ADT signal in 2005 associated with southerly increase has no counterpart in SST so that deeper thermal and/or salinity contributions must be suspected.

Thanks to these data sets, we confirm some previous results obtained from other authors and based on models or other data sets. For instance, the SST and zonal wind stress (τ^x) patterns we described for the two first SVDs with altimetry are quite similar to those observed by H06. However, we found that the meridional component of the wind stress -not only the zonal component- also plays a role in this variability. More surprising, if our results are in agreement with RB00's ones for the northern Atlantic SST and wind stress (but not for the southern hemisphere structures), our ADT and their 0-276m integrated heat content present different patterns. Again, these differences can result from different depth integrations and/or from salinity effects.

Finally, the dynamics involved in a possible teleconnection with the Pacific Ocean confirms the delay scheme and the regions evoked by Enfield and Mayer (1997, northern Atlantic, 1 month delay) and Tourre and White (2005, 16 months, equatorial region in the Gulf of Guinea) during the extreme ENSO-La Niña in 1997-98.

Because the 1992-2011 series we use covers 2 ENSO events of large amplitude in 1997-98 and in 2009-10, our next step will be to focus on these 2 periods, and in combination with model results, to investigate in more detail the variability and the connections between the Tropical Atlantic and Pacific Oceans. One of the pending question will be, as each of these events belong to one of the "eastern" or "central-Modoki" classifications, on the possibility to point out different responses in the tropical Atlantic.

Acknowledgements

This study was funded by the French CNES (Centre National d'Etudes Spatiales) and the IRD (Institut de Recherche pour le Développement) organizations.
Ssalto/Duacs altimeter products were produced by Ssalto/Duacs and distributed by Aviso, with support from Cnes (<http://www.aviso.oceanobs.com/duacs/>). We thank the AVISO group for helpful comments regarding these data sets.
We are grateful to the reviewers for their remarks and comments to improve the first version of this paper.
Sabine Arnault and Jean-Luc Mélice are supported by IRD.